Analysis of heliospheric disturbances during solar minimum using data of muon hodoscope URAGAN

D.A.Timashkov, N.S.Barbashina, D.V.Chernov, R.P.Kokoulin, K.G.Kompaniets, A.S.Mikhaylenko, A.A.Petrukhin, V.V.Shutenko, E.I.Yakovleva and I.I.Yashin

Moscow Engineering Physics Institute (State University), 115409, Russia

***Abstract*. Preliminary results of a two-year (2007-2008) monitoring of heliospheric disturbances by means of ground-based muon hodoscope URAGAN are presented. Total area of the setup is more than 34 sq. m. and angular muon track reconstruction accuracy is better than 1 degree, that allow study the muon flux dynamics from thousands of directions of celestial hemisphere with a good statistics. The projection of directions from muon hodoscope angular matrix to GSE coordinate system (taking into account geomagnetic field) gives possibility to observe heliospheric perturbations (ICME, shocks, magnetic clouds etc.) at large distances from the Earth using muon diagnostics technique. In some cases, the effects in "muon window" were observed many hours before the shock arrival to the Earth. The comparison with space-born detector data is also given.**

***Keywords*: muon diagnostics, heliospheric disturbances, interplanetary coronal mass ejections**

I. INTRODUCTION

Remote location of disturbances in solar wind (SW) and interplanetary magnetic field (IMF) propagating through the inner heliosphere is very actual and important problem of space weather researches [1]. To solve it, nowadays all-wave monitoring of the Sun or measurements of heliospheric conditions at some points in vicinity of the Earth are used. But information about the space between the Mercury's and the Earth's orbits is yet very scarce. One can point out two different approaches to receiving more information about this region. The first approach is based on an increase of the number of space-born instruments, positions of measurements of heliospheric environment. At present, STEREO mission will allow significantly widen possibilities of such space monitoring [2]. Another approach is based on the use of ground based cosmic ray detectors for space weather prediction purposes [3].

Usually, to detect secondary cosmic ray variations, the world-wide networks of neutron monitors or muon telescopes are used. New possibilities in this field are opened by the use of muon hodoscopes [4]. Unlike the neutron monitors, muon hodoscopes have higher counting rate, are sensitive to more energetic primary particles (up to hundreds GeV). Since muons (in contrast to neutrons) keep primary particle direction, the opportunity to measure the galactic cosmic ray variations from various directions appears. Moreover, muon hodoscope allows detect muons simultaneously from any direction of upper hemisphere and form "muon images" of disturbed regions.

This principle underlies the muon diagnostics: a new technique of remote monitoring based on the simultaneous detection of muon flux generated by high energy primary particles from various directions for the study of different dynamic processes in the heliosphere and near-terrestrial space [5]. In this approach, galactic cosmic rays are used as a natural source of penetrative radiation with a high level of constancy and isotropy. To study heliospheric disturbances it only remains to unroll a special "screen" which can detect cosmic rays in real time mode with sufficient angular resolution. Muon hodoscope URAGAN is a prototype of such a "screen" and gives possibility to test this approach. In this paper, preliminary results of monitoring of heliospheric disturbances during two years of solar minimum (2007-2008) by means of muon hodoscope URAGAN are presented and discussed.

II. URAGAN DATA PROCESSING

Description of muon hodoscope URAGAN can be found elsewhere [6]-[8]. URAGAN setup satisfies the main requirements to muon hodoscopes. It contains several coordinate planes equipped with two-coordinate data readout system. Such structure provides angular accuracy of muon track reconstruction better than 1° and ensures a high level of stability of muon detection efficiency. Total area of URAGAN is equal to 34.5 m^2 (three supermodules) and is sufficient to provide a good statistics: more than two hundred thousands muons per minute.

The supermodule response contains information about muon track in each of the X- and Y-projections. Two projected zenith angles are reconstructed in real time mode and are accumulated in 2D-directional matrices (zenith and azimuth angles, or pair of projected zenith angles); after that information about individual muon track is lost. Every minute these matrices are recorded on the hard disc.

Thus, the main format of muon hodoscope URAGAN data is two-dimensional muon angular matrix. To study muon flux fluctuations, for every cell of the angular matrix the average number of muons (estimated during preceding 24 hours and corrected for atmospheric pres-

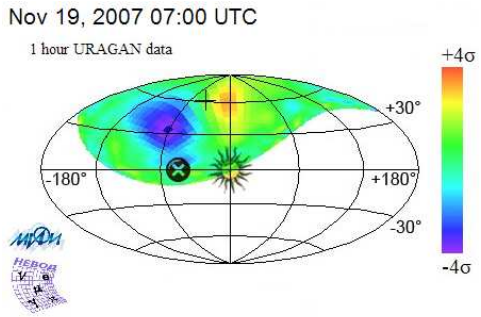

Fig. 1: Example of GSE-image obtained during passing of corotated interaction region near the Earth on November 19, 2007.

sure) is subtracted, and results are divided by standard deviations. Obtained data matrix is a muon photograph of the upper hemisphere with 1-minute exposure. Resolution of such muon images is determined by sizes of angular cells in URAGAN matrix data which is chosen as $2^\circ \times 2^\circ$ (in two projected zenith angles). The cell sizes are three times more than muon track reconstruction error in hodoscope.

To compare angular muon flux variations at ground level with variations of galactic cosmic rays in the heliosphere it is necessary to calculate asymptotic directions for each angular cell of muon matrix. These directions depend on geomagnetic coordinates of the detector, threshold energies of the setup (which for the URAGAN vary from 200 up to 600 MeV for different zenith angles) and average energies of galactic cosmic rays which give main contribution to URAGAN counting rate at given zenith angle. Procedure and results of calculations of asymptotic directions is described in [9].

Capabilities of muon hodoscope to measure the angular dynamics of muon intensity with unexcelled angular resolution open various ways for analysis of muon flux variations during heliospheric disturbances. Here we consider only two: GSE-images and anisotropy vector.

To obtain GSE-image, a "muon photograph" is projected to magnetopause using asymptotic directions and is transformed into GSE coordinate system. The example of GSE-images in "muon light" is shown in Fig. 1. A scale at the figure denotes values of muon intensity changes in standard deviation units. Circle with X-sign denotes the direction to IMF line (average GSE longitude is approximately equal to -45°). The Sun direction is pointed in the center of image. A thin cross denotes the asymptotic direction for vertical muons at observation point. Usually such image is obtained using one hour exposure.

For quantitative analysis, variations of parameters of local muon flux anisotropy are used. In a general case, muon flux intensity depends on both azimuth and zenith angle. Vector of local anisotropy describing preferred direction of muons arrival to ground level may be defined as mean of unit vectors pointing the directions of arrival of each detected muon. Using the numbers of muons detected in each angular cell of muon matrix, the projections of the anisotropy vector can be written in a following form:

$$A_X(t) = \frac{1}{M(t)} \sum_\theta \sum_\varphi N(\theta,\varphi,t) \cos\varphi \sin\theta \,,$$
$$A_Y(t) = \frac{1}{M(t)} \sum_\theta \sum_\varphi N(\theta,\varphi,t) \sin\varphi \sin\theta \,,$$
$$A_Z(t) = \frac{1}{M(t)} \sum_\theta \sum_\varphi N(\theta,\varphi,t) \cos\theta \,,$$

where t is the time, $N(\theta,\varphi,t)$ is the number of muons detected within angular cell (θ,φ), $M(t)$ is the total number of detected muons.

Since usually muon flux detected by means of URAGAN has systematical anisotropy caused by non-symmetry of setup acceptance and other reasons, along with vector $\vec{A}$ so called influence vector is used:

$$\vec{r} = \vec{A} - \langle \vec{A} \rangle,$$

where $\langle \vec{A} \rangle$ is a mean value of $\vec{A}$ over a long period (we used an interval Feb-Nov, 2007). The influence vector reflects real time changes of local anisotropy of muon flux caused by effects of any perturbations in near-Earth space or in the Earth atmosphere.

III. List of heliospheric disturbances

To choose periods of passing of disturbed regions in solar wind and IMF nearby the Earth the ACE data from OMNI database [10] have been analyzed. The following parameters were taken into account: magnitude of interplanetary magnetic field, velocity of solar wind, density and tempreture of solar wind. Signatures of disturbances are: increasing of magnetic field values and plasma velocity, sharp growths of solar wind and IMF parameters, typical turbulence behavior of magnetic field with fast solar wind or, on the contrary, regular behavior of magnetic field with reduced plasma density and temperature. Very often in the event different types of disturbances were observed. In the Table 1 selected periods of heliospheric disturbances (interplanetary CME, shocks, corotating interaction regions, magnetic clouds, etc) detected by ACE are listed. Some information about IMF and solar wind as well as about geomagnetic perturbations is also presented. The major part of the list is represented by disturbances caused by corotating interaction regions and is in a good agreement with CIR list over 2007-2008 composed by G.M.Mason et al. [11]. Since considered years fall on solar minimum amount of heliospheric disturbances is not very large (about 3 per month) and very strong space weather events did not happen (maximum Kp index is equal to 6.3, Dst index was not descend lower than -72). Against this background it is possible to select events with enlarged amplitude of variations of heliospheric or geomagnetic parameters ($B_{max} \geq 15$ nT, $V_{SW} \geq 650$ km/s, $Kp \geq 5$, $Dst \leq -50$ nT). If any two parameters in an event

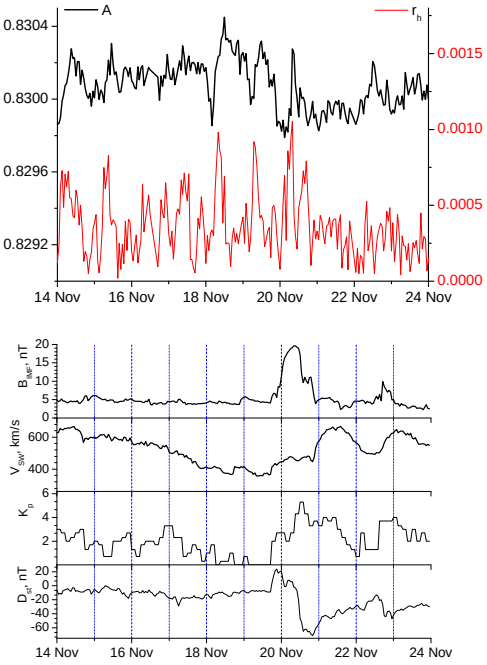

Fig. 2: Example of anisotropy vector variations (top) and heliospheric and geomagnetic data (bottom) during one of the events listed in Table 1.

exceeded these limits the event is marked as a moderate. There are 22 such events.

Last column in the table contains information about response of muon hodoscope on heliospheric disturbances. The basic signature of a perturbation in anisotropy vector behavior are: sharp peaks, increases of diurnal variations or long-time rises or declines of anisotropy values. The examples of reactions of muon flux on heliospheric perturbation are shown in Fig. 2. Here dependences of module of anisotropy vector (A) and horizontal projection of influence vector $r_h = \sqrt{r_x^2 + r_y^2}$ as well as variations of IMF value, SW velosity, Kp and Dst indexes are presented. It is clearly seen regular rises in A and three sharp peaks in r_h, first of which appeared approximately 40 hours before detection of this event by ACE.

Example of GSE-image of perturbation of cosmic ray flux in this event is presented in Fig. 1. This image corresponds to the second peak in r_h in Fig. 2. In order to remove the severe distortions of angular distribution of muon flux the special correction was introduced, which allowed to isolate the disturbances of the second order against the background of the large-scale distortions. The same method is used for constructing "muon images" of Forbush-decreases [12].

With the analysis of Table 1, attention is drawn to the fact that in the overwhelming majority of events effects were observed also in the data of muon hodoscope. Among 63 events, when URAGAN data exist, in 53 events (84 %) disturbances of anisotropy vector have been observed. Among 18 moderate events (with URAGAN data) the response in muon flux have been

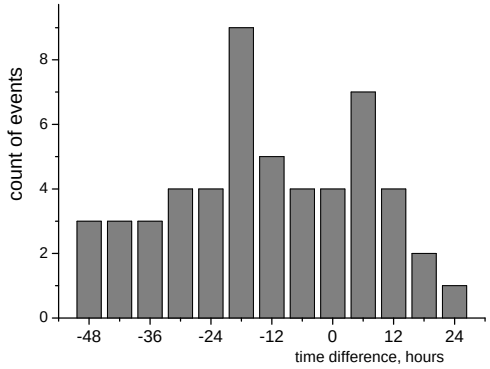

Fig. 3: Distribution in time difference between perturbation in ACE data and in URAGAN data.

detected in 17 ones. Also it is possible to note that perturbations in muon data were observed as a rule earlier than disturbance region arrived to the Earth. In Fig. 3, distribution of events in the difference of the onset time of perturbation in ACE and in URAGAN data is presented. The mean value of time shift is equal to -13.6 ± 2.6 hour.

IV. Conclusions

Construction of muon hodoscope and development of muon diagnostics open new possibilities of inner heliosphere monitoring by penetrative high energy particles. Preliminary analysis of heliospheric disturbances during 2007-2008 shows a rich potential of such method of space weather monitoring. No doubt, muon hodoscopes may as significantly extend capabilities of existing ground-level detector networks as be a basis of a new hodoscope network which will allow to conduct continuous monitoring of the heliosphere at a new level.

Acknowledgments

The research is performed at the Scientific and Educational Centre NEVOD with the support of the Federal Agency for Education, Federal Agency for Science and Innovations and RFBR (grant 08-02-01204-a).

References

[1] J.D.Richardson, Y. Liu, J.W.Belcher, Propagation and Evolution of ICMEs in solar wind, J.-A. Sauvaud and Z.Nemecek (eds.) Multiscale Processes in the Earth's Magnetosphere: From Interball to Cluster, 2004, p. 1.
[2] STEREO: http://stereo.gsfc.nasa.gov/
[3] L.I.Dorman, Ann. Geophys., **23**, 2005, p. 2997.
[4] V.V.Borog et al., Proc. 24th ICRC, Roma, **4**, 1995, p. 1291.
[5] D.A.Timashkov et al, Proc. 30th ICRC, Merida, **1**, 2007, p. 685.
[6] N.S.Barbashina, D.V.Chernov, R.P.Kokoulin, et al., Instr. Experim. Tech., **51**, 2008, p. 180.
[7] D.A.Timashkov, Yu.V.Balabin, N.S.Barbashina et al., Astroparticle Physics, **30**, 2008, p. 117.
[8] K.G.Kompaniets et al., Proc. 31 ICRC, Lodz, 2009, SH2.7, ID908.
[9] D.A.Timashkov et al., Proc. 21st ECRS, Koshice, 2008, ID4.04.
[10] OMNI database: http://omniweb.gsfc.nasa.gov/
[11] G.M. Mason, M.I. Desai, U. Mall at al., Solar Phys. **256**, 2009, p. 393.
[12] N.S.Barbashina et al., Proc. 31 ICRC, Lodz, 2009, SH2.6, ID887.

TABLE I: List of heliospheric disturbances

No	date & time	SSC	B_{max}, nT	V_{SW}, km/s	Kp	Dst	URAGAN response
1	Feb 12, 2007 10h	no	12.8	563	3.0	-18	no
2	Feb 13, 2007 12h	no	11.5	714	5.7	-32	yes, 13/02 04h
3	Feb 26, 2007 00h	no	12.2	428	3.3	-12	no
4	Feb 27, 2007 06h	no	13.4	647	4.3	-39	yes, 26/02 03h
5	Mar 6, 2007 05h	no	10.7	584	4.7	-26	yes, 04/03 12h
6	Mar 11, 2007 08h	no	10.4	698	5.0	-33	yes, 10/03 04h
7	Mar 23, 2007 04h	no	11.9	368	4.7	-69	yes, 24/03 03h
8	Mar 31, 2007 22h	no	10.6	561	5.0	-63	yes, 31/03 07h
9	Apr 08, 2007 23h	no	16.6	483	3.7	-8	yes, 08/04 10h
10	Apr 17, 2007 06h	no	10.2	393	3.3	-47	yes, 17/04 14h
11	Apr 22, 2007 02h	no	10.9	533	5.0	-28	yes, 20/04 03h
12	Apr 27, 2007 16h	no	9.0	633	5.0	-56	yes, 26/04 12h
13	May 7, 2007 08h	yes, 0826	19.5	643	5.0	-31	yes, 05/05 09h
14	May 18, 2007 03h	no	17.4	603	4.3	-5	yes, 18/05 10h
15	May 21, 2007 22h	yes, 2320 22/05 0555	13.3	459	4.3	-20	no data
16	May 23, 2007 02h	no	11.5	526	5.3	-63	no data
17	Jun 1, 2007 22h	no	11.6	443	2.3	7	yes, 01/06 02h
18	Jun 21, 2007 10h	no	9.8	556	4.0	-21	yes, 21/06 04h
19	Jun 29, 2007 18h	no	11.3	544	4.0	-11	yes, 28/06 21h
20	Jul 3, 2007 11h	no	10.3	620	4.3	-14	yes, 01/07 08h
21	Jul 10, 2007 18h	no	17.8	587	5.0	-40	yes, 10/07 00h
22	Jul 14, 2007 07h	no	12.8	603	5.3	-46	yes, 13/07 23h
23	Jul 20, 2007 04h	yes, 0412	10.9	539	4.0	-31	yes, 20/07 20h
24	Jul 29, 2007 01h	no	15.8	601	3.7	-19	yes, 27/07 20h
25	Aug 06, 2007 07h	no	16.3	684	5.7	-34	yes, 06/08 07h
26	Aug 10, 2007 10h	no	12.6	570	4.3	-32	no
27	Aug 25, 2007 10h	no	9.0	401	3.0	-8	yes, 26/08 06h
28	Aug 26, 2007 18h	no	18.4	672	4.0	-21	yes, 26/08 21h
29	Sep 1, 2007 22h	no	9.1	631	4.7	-22	no
30	Sep 14, 2007 15h	no	14.9	432	2.3	0	yes, 15/09 01h
31	Sep 20, 2007 10h	yes, 1012	10.5	482	4.0	-14	no
32	Sep 27, 2007 12h	yes, 1151	10.0	584	5.0	-24	yes, 27/09 16h
33	Oct 18, 2007 02h	no	13.0	672	4.0	-28	yes, 17/10 09h
34	Oct 25, 2007 11h	yes, 1135	14.9	692	4.7	-51	yes, 24/11 11h
35	Nov 12, 2007 22h	no	12.4	667	3.0	-12	yes, 11/11 04h
36	Nov 19, 2007 18h	yes, 1811	19.6	668	6	-71	yes, 18/11 02h
37	Dec 10, 2007 13h	no	15.7	634	4.3	-24	no data
38	Dec 17, 2007 03h	yes, 0253	15.9	687	4.0	-37	yes, 17/12 01h
39	Jan 4, 2008 23h	yes, 2250	15.9	662	4.0	-27	yes, 05/01 10h
40	Jan 24, 2008 22h	no	8.9	550	3.7	-17	yes, 24/01 02h
41	Jan 31, 2008 12h	yes, 1123	11.7	614	4.7	-44	yes, 31/01 09h
42	Feb 9, 2008 19h	no	16.9	725	4.7	-28	yes, 08/02 04h
43	Feb 18, 2008 12h	no	6.8	617	3.7	-27	yes, 17/02 02h
44	Feb 27, 2008 15h	no	10.5	768	5.3	-45	yes, 27/02 10h
45	Mar 8, 2008 08h	yes, 1142	15.9	701	5.7	-72	yes, 08/03 11h
46	Mar 26, 2008 03h	yes, 0936	9.5	676	5.0	-43	yes, 25/03 07h
47	Apr 4, 2008 11h	yes, 1503	12.2	709	5.0	-29	yes, 03/04 15h
48	Apr 16, 2008 10h	no	10.5	600	4.0	-24	yes, 14/04 22h
49	Apr 22, 2008 21h	no	11.8	654	5.3	-43	yes, 22/04 08h
50	Apr 30, 2008 16h	no	7.4	506	4.3	-12	no
51	May 28, 2008 02h	yes, 0225	9.7	531	3.3	-19	yes, 27/05 07h
52	Jun 14, 2008 12h	yes, 1223	14.8	658	5.7	-40	no data
53	Jun 19, 2008 22h	no	7.1	588	3.0	-31	no
54	Jun 24, 2008 20h	yes, 2010	8.2	391	2.7	-25	no
55	Jun 25, 2008 16h	no	13.4	639	4.0	-18	yes, 25/06 05h
56	Jul 5, 2008 11h	no	9.1	413	2.7	-12	yes, 05/07 18h
57	Jul 11, 2008 23h	yes, 12/07 0038	14.6	697	4.3	-40	no data
58	Jul 22, 2008 07h	no	9.7	640	4.0	-25	yes, 21/07 06h
59	Aug 8, 2008 23h	yes, 2344	18.3	645	5.3	-41	no data
60	Aug 18, 2008 03h	no	9.7	626	4.7	-26	no data
61	Sep 3, 2008 05h	yes, 1543	14.8	593	6.0	-51	no data
62	Sep 14, 2008 19h	yes, 15/09 1913	11.6	583	4.0	-29	no
63	Sep 30, 2008 13h	yes, 30/09 1234	8.2	705	4.0	-37	yes, 01/10 01h
64	Oct 11, 2008 06h	no	13.5	549	6.3	-60	no
65	Oct 28, 2008 06h	no	13.4	711	4.3	-24	yes, 27/10 06h
66	Nov 7, 2008 02h	yes, 0357	11.0	574	4.3	-30	yes, 07/11 03h
67	Nov 15, 2008 16h	yes, 1625	13.0	525	3.7	-31	yes, 16/11 04h
69	Nov 24, 2008 00h	yes, 24/11 2351	21.8	599	3.7	-7	yes, 22/11 17h
69	Dec 3, 2008 10h	no	9.4	502	3.3	-16	yes, 02/12 21h
70	Dec 16, 2008 11h	yes, 1159	9.5	370	2.7	-26	no data
71	Dec 22, 2008 16h	no	11.6	556	3.7	-25	yes, 21/12 20h
72	Dec 30, 2008 23h	no	12.2	525	3.3	-26	yes, 31/12 06h